Supporting Information

Catalytic Cracking of Yeast Borne Single Cell Oil for the Production of Small-Chain Olefins over Ptsn/Alumina Catalyst

Ankit Agrawal, [a,b,‡] Neha Bansal, [b,c,‡] Himanshu Raghav, [a,b] Arijit Jana,[c] Reena Goyal,[d] Debashish Ghosh, [b,c] Thallada Bhaskar, [b,c] Bipul Sarkar,*[a,b]

[a.] *Catalytic De-Polymerization Area, Upstream & Wax Rheology Division, CSIR-Indian Institute of Petroleum, Dehradun 248005, India*
Email – bsarkar@iip.res.in
[b.] *Academy of Scientific and Innovative Research (AcSIR), CSIR-HRDC Campus, Joggers Road, Kamla Nehru Nagar, Ghaziabad-201 002, India*
[c.] *Biochemistry and Biotechnology Area, Material Resource Efficiency Division, CSIR-Indian Institute of Petroleum, Dehradun-248005, India*
[d.] *Nanocatalysis Area, Light Stock Processing Division, CSIR-Indian Institute of Petroleum, Dehradun-248005, India*
‡ Equal contribution

Synthesis of SAPO-34 zeolite: The small pore zeolite was synthesised using the hydrothermal method as reported by Prakash *et al*.[4] In a typical synthesis of SAPO-34, 15.5 g of phosphoric acid was dissolved in 20 ml of deionised water, kept under stirring, and gently boiled until a clear solution was visible. While stirring, 9.2 g $Al(OH)_3$ was added to the phosphoric acid solution. To the resulting mixture of $Al(OH)_3$ and phosphoric acid further 10 ml H_2O was added and stirring continued for another 7 h. In another beaker, 4 g LUDOX-AS40, 12 g morpholine and 15 ml water were added. Then, the colloidal silica solution was added dropwise into the Al(OH)3 solution, and another 25 mL of water was added. The complete solution was then stirred vigorously for 7 hours. After stirring, the solution was heated at a mild temperature, i.e. Aged at 40℃ for 24 hours. Then whole solution was kept for hydrothermal treatment in a Teflon-lined autoclave at 200°C for 24 h. After the hydrothermal treatment, the autoclave was allowed to cool to RT. The resulting white material was filtered off, washed thoroughly with deionised water, and placed in the oven overnight. After oven drying, the catalysts were calcined at 550°C for 4 h at a ramp rate of 2.5°C/min.

Synthesis of 1% Pt supported γ-alumina: The monometallic catalyst was prepared via the wet impregnation method. The Pt/Al_2O_3 was prepared using $[Pt(NH_3)_4](NO_3)_2$, the precursor to the Pt. First, $[Pt(NH_3)_4](NO_3)_2$ (0.3 mmol) was dissolved in 10 mL of deionised water. 1.5 mmol of CTAB (1:1, metal:CTAB) was separately dissolved in 10 mL of deionised water. Both solutions were vigorously stirred at 60°C and then they were slowly added to 5 g of alumina (powder) and the whole mixture was kept under continuous stirring for the next 3 h. The mixture was aged in a forced air oven at 80°C overnight and

dried while slowly allowing water to evaporate. The light gray powder obtained was ground and calcined at 650°C for 4 h with a slow ramp rate of 1.25°C/min.

Biomass pre-treatment, yeast cultivation, and SCO production: The lignocellulosic biomass, sugarcane bagasse (SCB) was dried and reduced to a particle size of <5 mm by grinding. The hemi-cellulosic fraction (C_5) was extracted through acid hydrolysis as per our previous reports[1]. In brief, SCB was digested with sulphuric acid (3.76% w/w) in a 1:10 solid to liquid ratio for 90 minutes, at 140ºC under an autogenous pressure followed by neutralisation (to pH 4.5) with CaO. The acid treated C_5 (mainly xylose) enriched stream was further filtered and analysed through HPLC. A xylose content of 20.0 ± 1.3 g/L and a negligible ~ 0.78 g/L of glucose was reported along with biomass inhibitors; acetic acid and furfural with a composition of ~1.28 g/L and ~15 mM respectively. The C_5 enriched stream supplemented with salts (composition in g/L; 20, C_5 hydrolysate with adjusted synthetic xylose; 1.98, $(NH_4)_2SO_4$; 1.26, KH_2PO_4; 0.748, Na_2HPO_4; 0.7, $MgSO_4$; 1, yeast extract; 0.05, $CaCl_2$; 0.005, H_3BO_3; 0.005, $MnSO_4$; 0.005, NH_4MoO_4; 0.005, $CoNO_3$; pH 4.5) at 32ºC under high aeration was used for RMIIPL32 cultivation. For bulk RMIIPL32 SCO production, fermentation was carried out in a 15 L *in-situ* stirred tank bioreactor (Andel BioSac, India) with an automated SCADA system through a fed-batch model as reported earlier[2,3]. Matured yeast cells were harvested, oven-dried (60ºC), and pulverised through grinding. The pulverised RMIIPL32 biomass was subjected to Soxhlet mediated (Chloroform: Methanol, 2:1 v/v) lipid extraction. The extracted lipid was concentrated to remove solvent and washed with n-hexane to separate out non-polar lipid. The concentrated yeast lipid was analysed through gas chromatography as described in earlier studies[1, 2] and used for olefin conversion. The entire process (cradle to gate) of SCO production and recovery from lignocellulosic biomass derived pentose sugars emit green house gas, which is under permissible limit (Cradle to gate life cycle impact assessment of yeast SCO derived from cane sugar bagasse's pentosan) as per our earlier report.[1]

Table S1. The synthesised catalysts with catalyst codes, support used and the metal contents.

Catalyst	Pt		Sn		Zeolite Support
	Pt (%)	Amount of metal precursor (mmol)	Sn (%)	Amount of metal precursor (mmol)	
0.5Pt/CHA	0.5	0.15	0	0	SAPO-34
0.5Pt/BEA	0.5	0.15	0	0	β zeolite
0.5Pt/Al_2O_3	0.5	0.15	0	0	γ alumina
1Pt/Al_2O_3	1	0.3	0	0	γ alumina
1Pt10Sn/Al_2O_3	1	0.3	10	4.2	γ alumina

Table S2. Physico-chemical characterization of yeast SCO

Density (45◦C) (kg/m^3)	0.906		
Kinematic viscosity (45◦C) (mm^3/s)	26.62		
FAME (Fatty Acid Methyl Ester) analysis			
Fatty acid methyl esters	Molecular Formulas	Numerical representation	Composition (%wt)*
Methyl cis-10 pentadecenoate	$C_{16}H_{30}O_2$	C 15:1	11.04
Methyl Palmitate	$C_{16}H_{32}O_2$	C 16:0	11.37
Methyl Palmitoleate	$C_{16}H_{30}O_2$	C 16:1	5.95
Methyl stearate	$C_{18}H_{36}O_2$	C 18:0	1.95
Methyl cis-9 oleate	$C_{18}H_{34}O_2$	C 18:1	13.02
Methyl Linoleate	$C_{18}H_{32}O_2$	C 18:2	28.84
Methyl Linolenate	$C_{18}H_{30}O_2$	C 18:3	3.14
cis-5,8,11,14 ETA	$C_{20}H_{32}O_2$	C 20:4	1.46
Acid Value, saponification value, Iodine number, pour point		**Elemental analysis (in wt.%)**	
acid value (TAN) (mg KOH/g)	44.68	C	66.24
saponification value (mg KOH/g)	159.9	H	9.16
iodine number (mg of I_2/100g)	83.84	N	7.79
pour point (^{o}C)	-5.74	S	-
Elemental analysis was carried out in a CHNS analyser; Anton Paar- refractometer; Anton Paar, SVM3000-Stabinger-ASTM-D7042;			

Table S3. The rate of methanation of various catalysts shown in Table 1

Catalyst	TOF (h^{-1})	Liquid yield (%)	Gas Yield (%)	$R_{methane}$ ($m_{methane}/m_{active\ sites}/h$)
0.5Pt/CHA	1330.77	41.70	58.30	833.33
0.5Pt/BEA	1382.05	47.22	52.78	741.02
0.5Pt/Al_2O_3	1576.92	11.00	89.00	633.33
1Pt/Al_2O_3	801.28	5.55	94.45	274.35
1Pt10Sn/Al_2O_3	47.01	6.94	93.06	15.09
1Pt10Sn-Al_2O_3b	45.81	8.50	91.50	15.02
1Pt10Sn/Al_2O_3c	12.60	7.00	93.00	14.57

Table S4. Product phases in up-gradation of SCO over various catalysts

Catalyst	Liquid yield (%)	Gas Yield (%)
0.5Pt/CHA	41.70	58.30
0.5Pt/BEA	47.22	52.78
0.5Pt/Al_2O_3	11.00	89.00
1Pt/Al_2O_3	5.55	94.45
1Pt10Sn/Al_2O_3	6.94	93.06
1Pt10Sn-Al_2O_3[a]	8.50	91.50
1Pt10Sn/Al_2O_3[b]	7.00	93.00

TOF expressed as moles of to CO_2 per mole of surface Pt atoms per minute was calculated. It appears that the TOF at 120 and 160 °C was almost identical in the entire range of Pt dispersion, suggesting "structure–insensitive reaction" over Pt/Al_2O_3.

Table S5. Product distribution table for gaseous products over 1Pt10Sn/Al_2O_3 (Quantification done in RGA)

S. No.	Component	Carbon no.	Vol (%)[a]
1	H_2	0	20.9
2	O_2	0	1.3
3	CO/CO_2	1	4.20
4	Methane	1	25.18
5	Ethane	2	6.99
6	Ethylene	2	41.50
7	Propane	3	0.56
8	Propylene	3	15.85
9	1-butene	4	2.33
10	1,3-butadiene	4	2.98
11	trans-2-butene	4	0.23
12	cis-2-butene	4	0.16

[†] Reaction conditions: Catalyst wt-0.5 g (pelletized), Temp-600°C, LHSV-2.4 h^{-1}, GHSV-2400 h^{-1}, Time-3h.

[a] Volume has been normalized wrt carbon containing components

[b] Total gas yield = 94%

Table S6. Comparison presenting evidence of a significant advance for sustainable production of green olefins (as per the editorial by Prof. Philip Jessop)[3]

Process	Feed	Risk type	Metric	Merits	Ref.
Steam cracking	Naphtha	• Energy usage/ global warming • Water consumption • Resource depletion	Process runs at high temperature (>600℃) and water usage ~0.35-0.5 bbl water/bbl feed CO_2 emission: 300 MT/pa	Widely used processes, optimised in the existing conditions	[4, 5]
Fluid catalytic cracking	Vacuum gas oil (VGO)	• Energy usage/global warming • Resource depletion	Process runs at high temperature (~650℃)	2nd most established olefin production process, shares ~30% of total olefin production	[6-8]
Vis-breaker	Vacuum residue	• Resource depletion	Resource or feed consumption is more	Runs at relatively low temperature	[9, 10]
Dehydro genation	Paraffin	• Energy usage/global warming • Human toxicity • Resource depletion	1. Process runs at high temperature (~580-650℃) 2. Use of hazardous metal e.g., Cr (it remains in three oxidation states III, V, VI). Among these 3 oxidation states V, VI cause toxicity in environment and human nervous system. However, the trivalent state is non-toxic in nature.	Abundance of shale gas reservoirs makes this process viable and economic	[11, 12]
Catalytic cracking	Single cell oil (SCO)	• Feed availability • Available technology	The end-products are separable in the current refinery setup	Lower carbon footprint/unit of olefin produced**	This study

**LCA analysis of Yeast lipid-based aromatics, biofuels and oleochemicals from lignocellulosic biomass has been detailed in our earlier work in RSC Sustainable Energy Fuels, 2020,4, 387-398.[1]

Table S7. Product distribution table for liquid products over 1Pt10Sn/Al_2O_3 (Quantification done in DHA)

Carbon No.	Paraffins Vol (%)[a]	i-Paraffins Vol (%)[a]	Olefins Vol (%)[a]	Naphthenes Vol (%)[a]	Aromatics Vol (%)[a]	Total Vol (%)[a]
C1	0.00	0.00	0.00	0.00	0.00	0.00
C2	14.51	0.00	2.37	0.00	0.00	16.87
C3	0.12	0.00	0.00	0.00	0.00	0.12
C4	0.06	2.01	3.00	0.00	0.00	5.06
C5	0.05	1.85	3.85	0.00	0.00	5.75
C6	0.23	0.84	3.42	0.00	0.73	5.22
C7	0.21	0.06	2.54	0.21	0.51	3.53
C8	0.20	0.69	0.89	0.33	0.38	2.49
C9	0.17	0.66	1.58	0.31	0.23	2.95
C10	0.00	0.17	0.00	0.75	0.40	1.32
C11	0.27	1.20	0.71	0.00	1.22	3.41
C12	15.41	0.00	0.00	0.28	1.19	16.89
C13	0.11	0.00	0.38	0.00	0.00	0.49
C14	0.57	0.00	0.75	0.00	0.00	1.32
C15	1.51	0.00	0.00	0.00	0.00	1.51
C16	0.39	0.00	0.00	0.00	0.00	0.39
C17	0.49	0.00	0.00	0.00	0.00	0.49
C18	0.09	0.00	0.19	0.00	0.00	0.28
C19	0.00	0.00	0.55	0.00	0.00	0.55
Total	34.41	7.48	20.22	1.88	4.66	68.66

† Reaction conditions: Catalyst wt-0.5 g (pelletized), Temp-600°C, LHSV-2.4 h^{-1}, GHSV-2400 h^{-1}, Time-3h.

[a] Volume has been normalized wrt carbon containing components

[b] Total liquid yield = 6%

[c] Oxygenates – 0.0516%, Unknows – 14.03%, C20+ – 16.32%

Table S8. Total acidity and Brønsted and Lewis acid sites of the catalyst

Catalyst	NH_3-TPD	Pyridine IR			
	(mmol.g^{-1})	B (mmol.g^{-1})	L (mmol.g^{-1})	B+L (mmol.g^{-1})	B/L
Alumina	0.26	0.205	0.02	0.225	10.25
1Pt10Sn/$Al_2O_3^{Fresh}$	0.22	0.135	0.031	0.166	4.35
1Pt10Sn/$Al_2O_3^{Spent}$	0.09	0.121	0.008	0.129	15.12

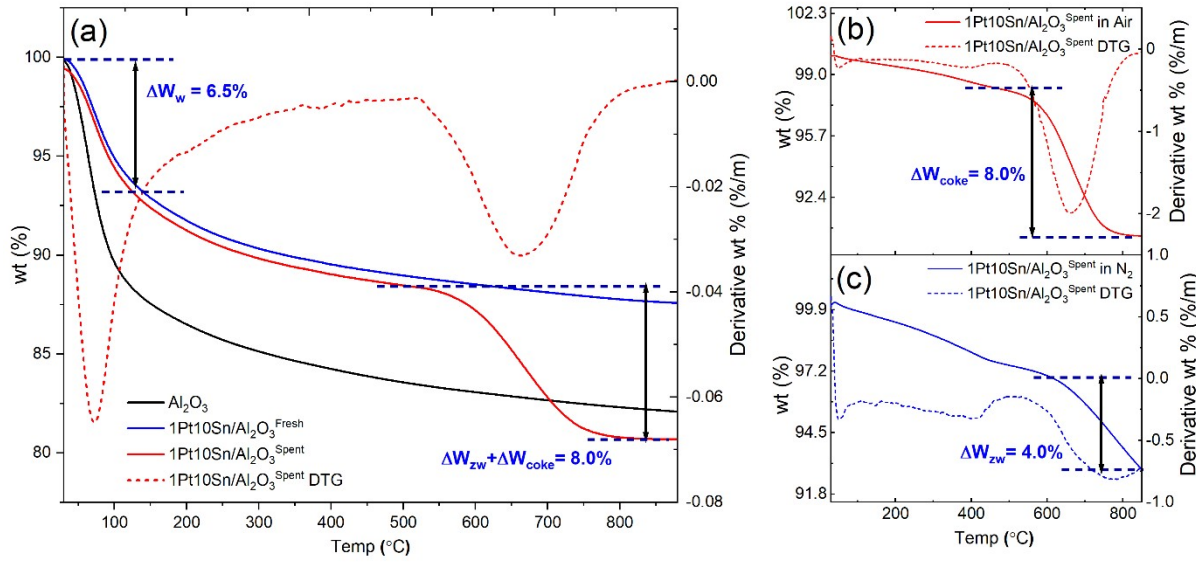

Figure S1. (a) TGA profile of γ-alumina, $1Pt10Sn/Al_2O_3^{Fresh}$ and $1Pt10Sn/Al_2O_3^{Spent}$ (b) and (c) are the TGA analysis in air and N_2 environment.

A sharp weight loss (~12.3%) at 100℃ was observed in the TGA, corresponding to the moisture loss from the alumina surface. However, the weight loss was significantly decreased (~6.5%) when the Pt and Sn were loaded on the γ-alumina surface. This decrease in the moisture absorption capability confirms that the metal loading made the γ-alumina surface much more stable toward H_2O poisoning.[5,6] It can be assumed that the interaction of Pt and Sn with the γ-alumina framework filled the -OH valency, making the catalytic surface less moisture-prone. TGA was carried out in N_2 atmosphere (Figure S1c) to verify the presence of zeolitic water in the catalyst. The results indicate a presence of zeolitic water in the framework as there was a reflection in the weight loss between 600-800°C (Figure S1b). After confirming the presence of zeolitic water, the same catalyst was further heated in the air environment. Figure S1b shows that there was a weight loss (~8.0%) between 600-800℃, which confirmed the presence of graphitic carbon which converted into CO/CO_2 and resulted in the sharp weight loss.

Zeolitic water in the catalyst caused a sharp weight loss at 100°C, corresponding to the evaporation of water molecules from the catalyst surface. It can be assumed that the interaction of Pt and Sn with the γ-alumina framework filled the OH valency which made the catalytic surface less moisture-prone. Figure S1b shows that there was a weight loss between 600-800°C which confirmed the presence of graphitic carbon converted into CO/CO2. This decrease in the moisture absorption capability confirms that the metal loading made the γ-alumina surface much more stable toward H_2O poisoning.

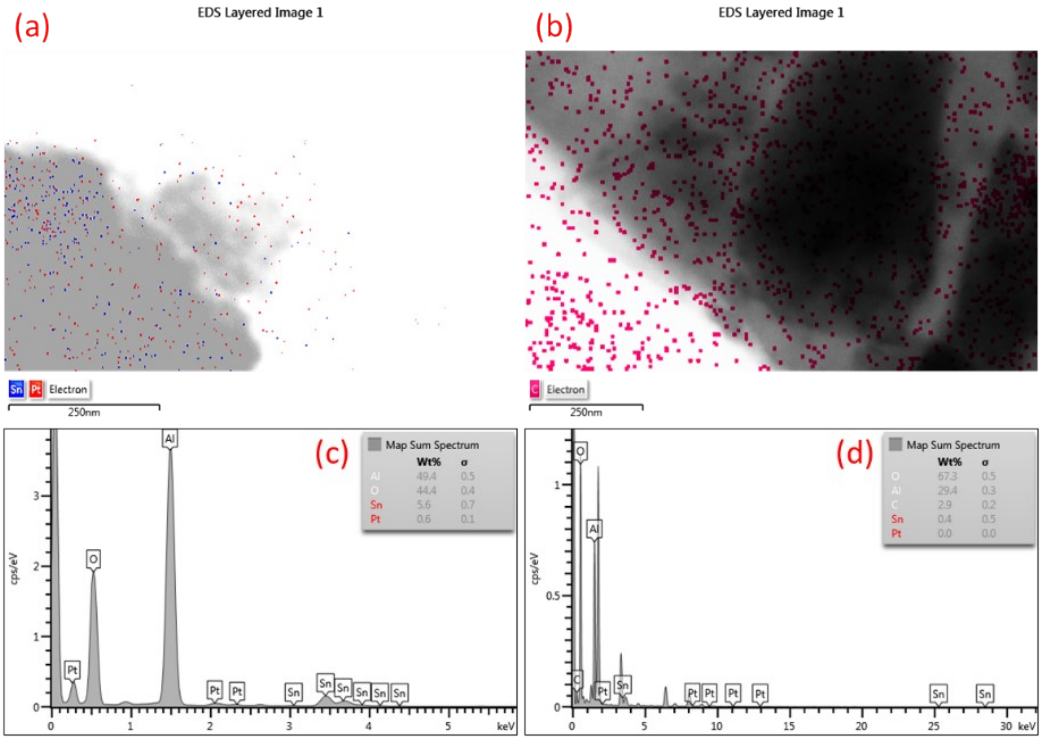

Figure S2. (a) & (c) EDX elemental mapping and elemental quantification of 1Pt10Sn/$Al_2O_3^{Fresh}$ for Pt and Sn metals, (b) and (d) EDX elemental mapping and elemental quantification of 1Pt10Sn/$Al_2O_3^{Spent}$ for carbon deposition.

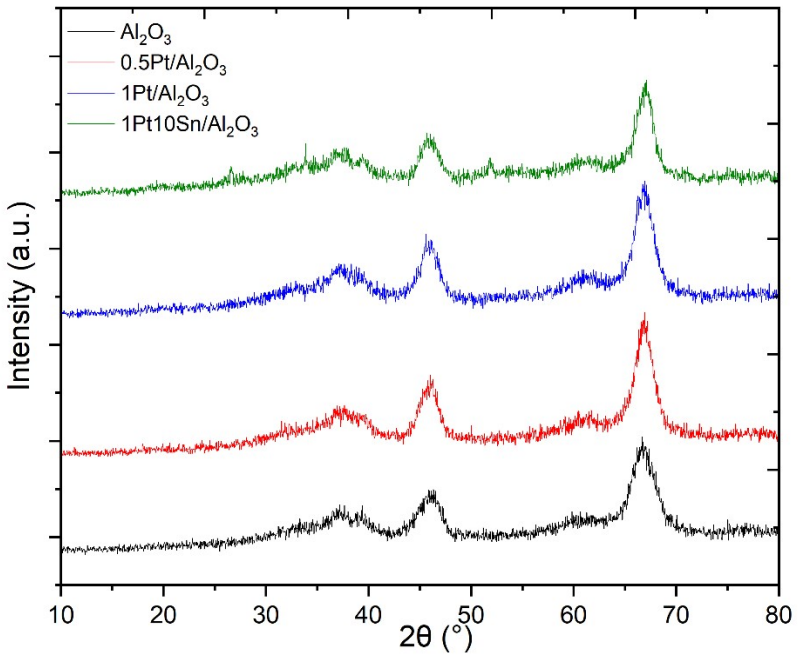

Figure S3. Powder X-ray diffraction pattern of the as synthesised catalysts

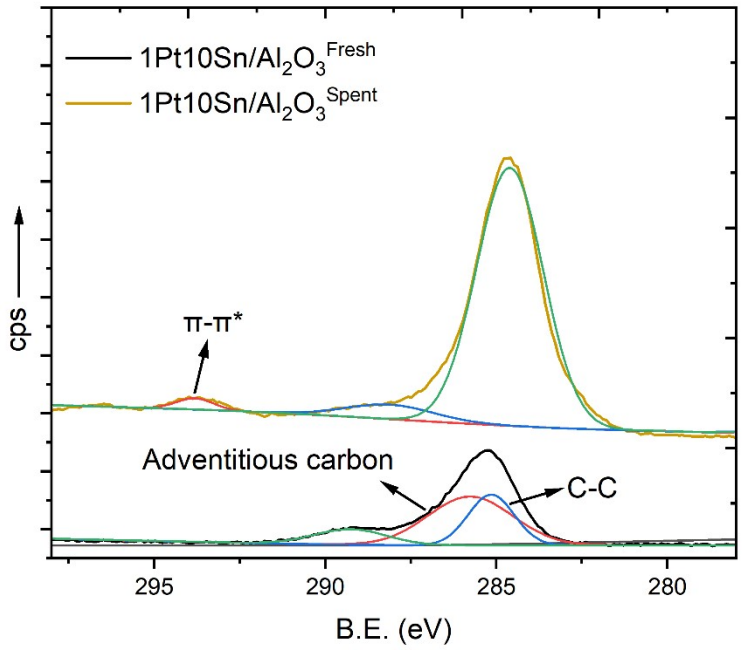

Figure S4. C1s XP spectra of fresh and spent catalysts

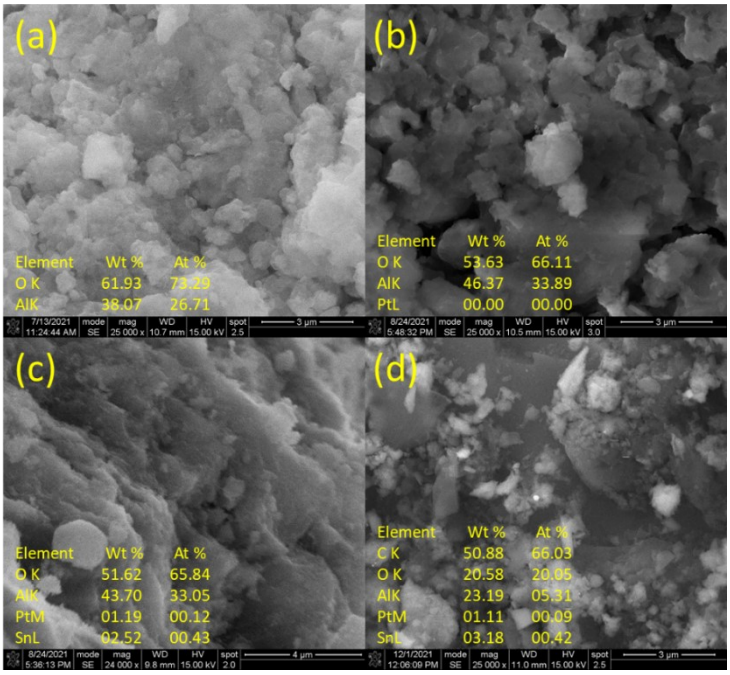

Figure S5. SEM images of (a) alumina, (b) 1Pt/Al_2O_3, (c) 1Pt10Sn/$Al_2O_3^{Fresh}$ and (d) 1Pt10Sn/$Al_2O_3^{Spent}$. Elemental quantification table (EDAX) has been shown on their respective images.

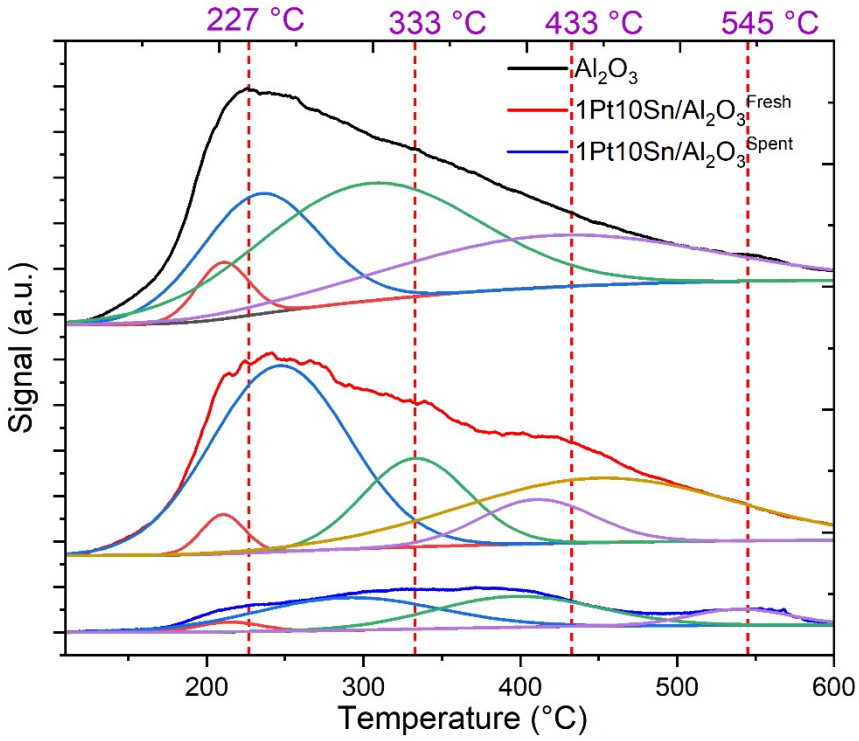

Figure S6. NH_3-TPD of γ-alumina, fresh and spent catalysts.

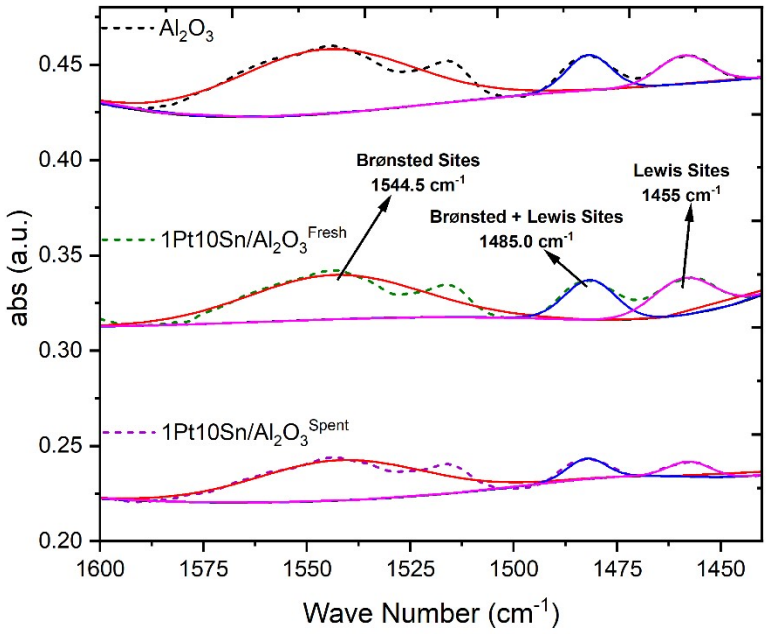

Figure S7. Pyridine adsorbed I.R. spectra of γ-alumina, fresh and spent catalysts.

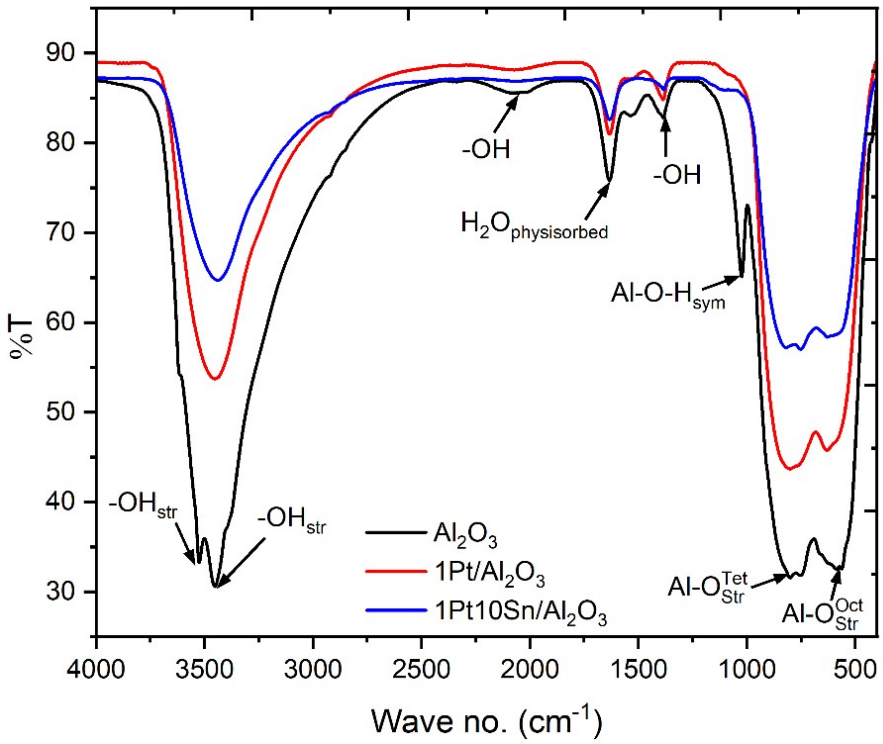

Figure S8. FT-IR spectra of the as synthesised catalysts.

The Fourier transformed-infrared spectrum of support, $1Pt/Al_2O_3$, and $1Pt10Sn/Al_2O_3$ are shown in Figure S8. The I.R. vibration in the range of 500-900 cm^{-1} attributes to Tetrahedral and octahedral Al-O stretching. The I.R. vibrational peak at ~1100 cm^{-1} depicts the Al-O-H symmetric stretching. This band at ~1100 cm^{-1} completely vanished when the Pt and Sn metals were loaded. This implies that Al-O-M interaction replaced the -O.H. group from the γ-alumina framework. Therefore, there was a significant reduction in the -O.H. vibrations across the full I.R. spectrum. This can be justified by the TGA curve which showed less water quantity at ~110℃. The stretching vibrations at 3450 cm^{-1} can be referred to as -O.H. group present in the form of external water absorbed in the zeolitic framework. However, the physiosorbed water is still present in all the catalyst at ~1700 cm^{-1}. The presence of zeolitic water can be observed in TGA profile which was run in N_2 environment (Figure S1c).

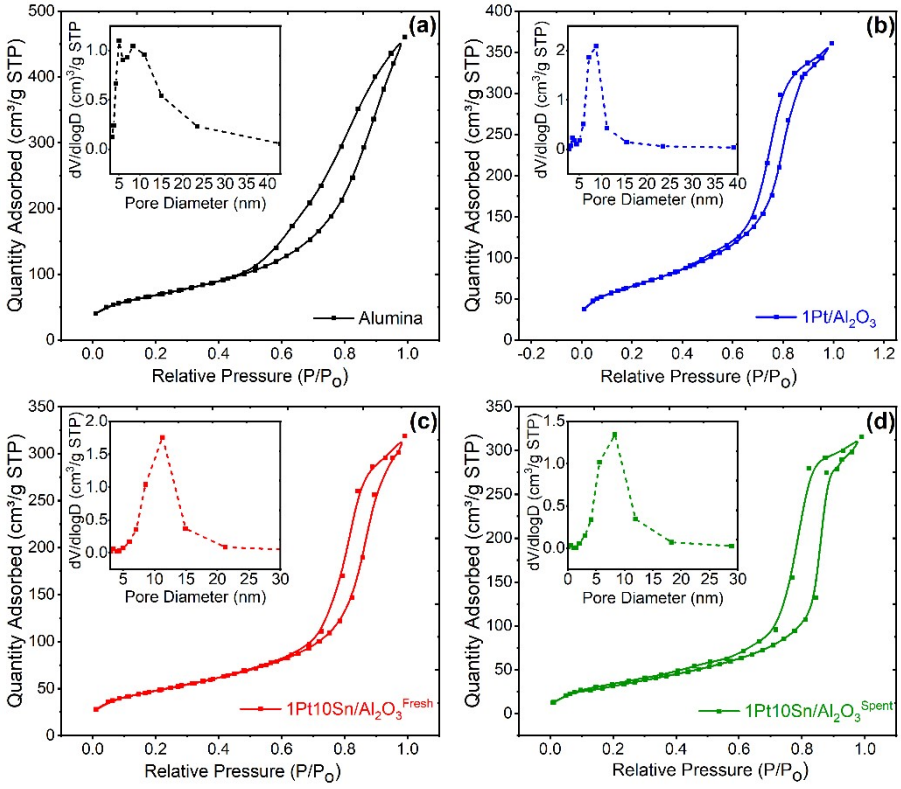

Figure S9. N2-adsorption-desorption hysteresis loop and pore size distribution curve (inset) of (a) γ-alumina, (b) $1Pt/Al_2O_3$, (c) $1Pt10Sn/Al_2O_3^{Fresh}$ and (d) $1Pt10Sn/Al_2O_3^{Spent}$

The N_2 adsorption-desorption hysteresis curve of γ-alumina and metal-loaded γ-alumina catalysts heat-treated at 200°C in vacuo are shown in a representative Figure S9. The physical properties of synthesised catalysts obtained from BET analysis and pore size distribution calculations using N_2-desorption data are tabulated in Table 2. A careful observation of the hysteresis loop of the N_2-adsorption-desorption (Figure S9) and the porosity of the catalysts **(Table 2)** shows that the metal loading on the γ-alumina surface has a profound influence on the surface area and the pore structure of the catalyst.

From the Pore diameter vs pore volume curve, it is visible that the average pore size falls in the range of 5-10 nm. However, the adsorbed quantity of the N_2 significantly decreased after metal loading, which suggests that the impregnation of metal particles covered the accessible pores of the γ-alumina surface. The same property can be observed in **Table 2** i.e. the surface area (S_{BET}) is slightly reduced without significant change in the pore diameter of the catalyst.

In the final catalyst, which is fresh $1Pt10Sn/Al_2O_3$, the BET surface area decreased drastically, and it can be assumed that the Pt and Sn covered most of the available pores of the surface and uniformly distributed over the alumina. The surface area further decreased in the recovered catalyst from the reaction denoted as $1Pt10Sn/Al_2O_3$Spent, mainly due to coke deposition during the cracking reaction.

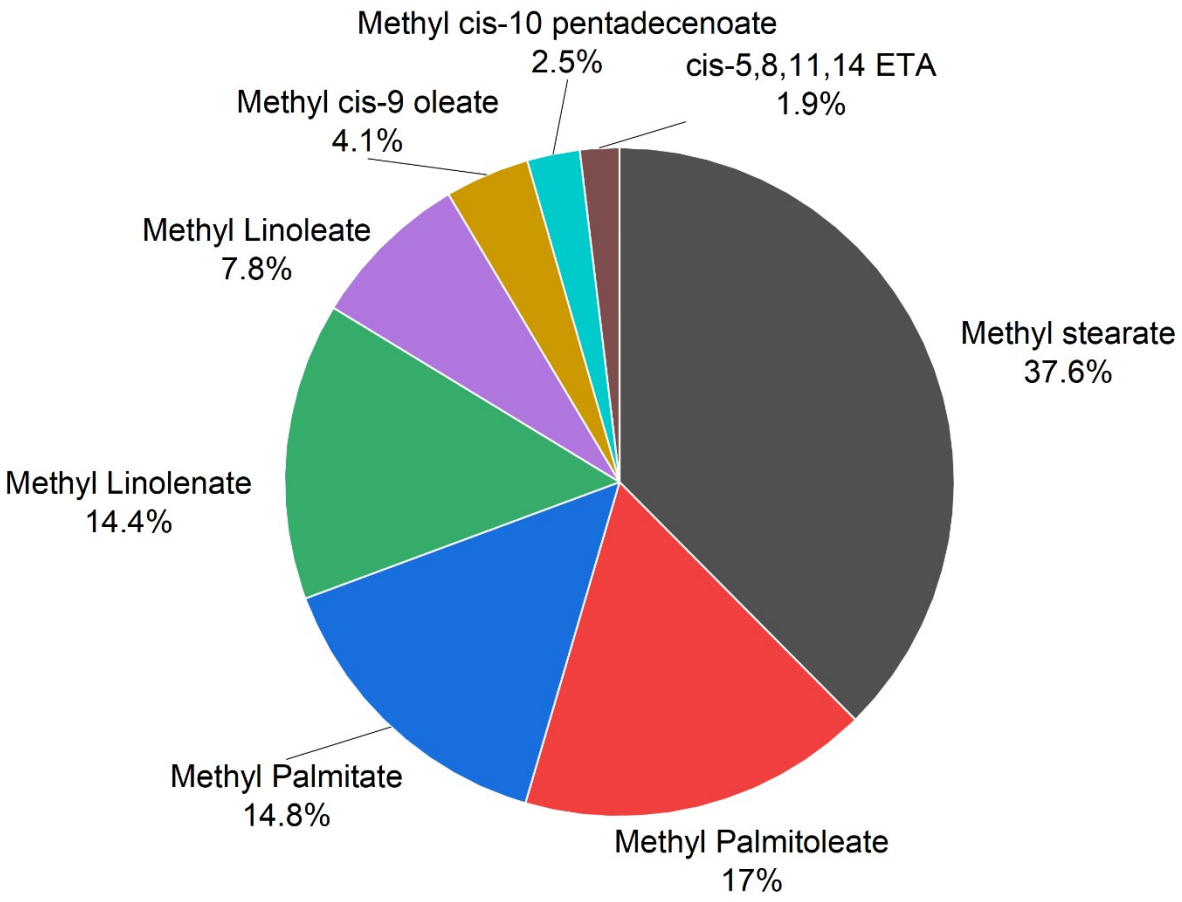

Figure S10. The fatty acid methyl ester profile of yeast SCO.

1. T. Sharma, D. Dasgupta, J. Singh, T. Bhaskar and D. Ghosh, *Sustainable Energy & Fuels*, 2020, **4**, 387-398.
2. O. Singh, T. Sharma, I. Ghosh, D. Dasgupta, B. P. Vempatapu, S. Hazra, A. L. Kustov, B. Sarkar and D. Ghosh, *ACS Sustainable Chemistry & Engineering*, 2019, **7**, 13437-13445.
3. P. Jessop, *Green Chemistry*, 2020, **22**, 13-15.
4. P. Sun, A. Elgowainy, M. Wang, J. Han and R. J. Henderson, *Fuel*, 2018, **221**, 542-557.
5. I. Amghizar, J. N. Dedeyne, D. J. Brown, G. B. Marin and K. M. Van Geem, *Reaction Chemistry & Engineering*, 2020, **5**, 239-257.
6. M. F. Alotibi, B. A. Alshammari, M. H. Alotaibi, F. M. Alotaibi, S. Alshihri, R. M. Navarro and J. L. G. Fierro, *Catalysis Surveys from Asia*, 2019, **24**, 1-10.
7. D. D. Miller, M. Smith and D. Shekhawat, *Fuel*, 2020, **259**, 116239.
8. A. I. Hussain, A. M. Aitani, M. Kubů, J. Čejka and S. Al-Khattaf, *Fuel*, 2016, **167**, 226-239.
9. A. de Klerk, *Energ Fuel*, 2020, **34**, 15285-15298.
10. L. Wang, A. Zachariah, S. Yang, V. Prasad and A. de Klerk, *Energ Fuel*, 2014, **28**, 5014-5022.
11. J. J. Sattler, J. Ruiz-Martinez, E. Santillan-Jimenez and B. M. Weckhuysen, *Chem Rev*, 2014, **114**, 10613-10653.
12. A. Węgrzyniak, S. Jarczewski, A. Węgrzynowicz, B. Michorczyk, P. Kuśtrowski and P. Michorczyk, *Nanomaterials*, 2017, **7**.